Wavelet and Cross-Correlation Analysis of Relativistic Electron Flux with Sunspot Number, Solar Flux, and Solar Wind Parameters

P. Poudel, N. Parajuli, A. Gautam, D. Sapkota, H. Adhikari, B. Adhikari, A. Silwal, S. P. Gautam, M. Karki, R. K. Mishra

Wavelet and Cross-Correlation Analysis of Relativistic Electron Flux with Sunspot Number, Solar Flux, and Solar Wind Parameters

P. Poudel[1,*], N. Parajuli[1], A. Gautam[2], D. Sapkota[3], H. Adhikari[4], B. Adhikari[1, 5],
A. Silwal[1], S. P. Gautam[6], M. Karki[4], R. K. Mishra[5]

[1]Department of Physics, Patan Multiple Campus, Lalitpur, Nepal

[2]Birendra Multiple Campus, Chitwan, Nepal

[3]Tri-Chandra Multiple Campus, Kathmandu, Nepal

[4]Amrit Campus, Kathmandu, Nepal

[5]Department of Physics, St. Xavier's College, Kathmandu, Nepal

[6]Central Department of Physics, Tribhuvan University, Kathmandu,Nepal

[*]Corresponding Email: prakashpdl70@gmail.com

Abstract

The Geostationary Operational Environmental Satellites (GOES) have been monitoring the Earth's radiation environment and is providing the electron flux data (of energy >0.8 MeV, >2 MeV, and >4 MeV) by means of a connected sensor subsystem. Relativistic electron flux is one of the components of the radiation belt which not only affects the electrical system in satellites but also has an impact on Earth's upper atmospheric climatic variation. We have carried out a study to determine the relation of sunspot number (R), solar flux (F10.7), and solar wind parameters i.e., solar wind velocity (Vsw), plasma density Nsw), the southern component of the interplanetary magnetic field (IMF-Bz), Plasma temperature (Tsw) with relativistic electron flux of energy >0.8 MeV, >2 MeV, and >4 MeV in outer radiation belt using the data of 24 years (1996-2020) covering solar cycle 23 and 24. Time series analysis, Cross-correlation and wavelet analysis techniques have been used in this study. The time series plot displayed that the radiation is occupied mostly by electron flux of energy less than 4 Mev and solar cycle 23 (1996-2008) was strong to produce more intensity of relativistic electron flux of all energy in comparison to cycle 24 (2008-2019). Results from cross-correlation analysis illustrated that Bz has no significant impact on the enhancement of relativistic electron flux of any energy range in the radiation belt. Whereas other studied parameters have a positive correlation with relativistic electron flux, but with significantly different coefficient values for different energy. We found that electron flux >0.8 MeV and >2 MeV has a strong positive association with sunspot number, solar flux, solar wind velocity, plasma density and temperature whereas weak correlation with electron flux of energy >4 MeV. This result leads us to conclude that solar activity and solar parameters have greater influence in producing relativistic electron flux of energy ~ 0.8-4 MeV, than of flux > 4 MeV. The study made to observe the distribution of relativistic electrons in radiation belt with time through continuous wavelet analysis showed that electron flux of energy >0.8 has a higher periodicity in comparison to the flux of other energy ranger.

Keywords: Continuous Wavelet Transform, Cross-Correlation, Solar Wind Parameters, Sunspot Number, Relativistic Electron Flux.

1. INTRODUCTION

The instability in Sun's magnetic field causes a powerful eruption of plasma bubbles and clouds of magnetic fields from the sun's surface in interplanetary space known as coronal mass ejection (CME). When these erupted structures,

mostly possessing charged particles hit our Planet, they get trapped in Earth's magnetic field forming a radiation belt in the magnetosphere called as Van Allen radiation belt [1, 2]. Van Allen radiation belt covering the height around 3Re to 10Re consists of relativistic electrons and protons and most of the artificial satellites operates in this belt region [3]. The energetic electrons of this radiation belt are sometimes called killer electrons because they potentially harm satellites causing satellite anomalies through dielectric charging [4, 5]. Due to the increasing importance of satellite and space technology for human well-being (communication, navigation, safety and emergency management, Earth observation, etc.), the research on radiation belt and relativistic electrons have received the considerable attention over last few decades. [6, 7, 8].

For the first time, the relativistic electrons of MeV energy were directly detected by Meyer and Vogt from solar proton flares by balloon observation [9]. Taking account of various processes, after being ejected into solar atmosphere with solar proton flares, both components of proton and electron diffuses into the outer space [10]. Having a negligible amount of energy loss while interacting with solar plasma, proton accelerates [11]. But in contrary to it, electron components decelerate as it loses a surplus amount of energy through ionization and synchrotron radiation [10].

Various researchers have studied the relation of relativistic electrons with other solar parameters and geomagnetic indices using different statistical tools and instruments. In 1979, George Paulikas and Bern Blake showed a correlation between solar wind velocity (Vsw) and geosynchronous relativistic electron fluxes which became the landmark on the study of radiation belt [12]. Paulikas & Blake (1979), Blake et al. (1997) provided results about the continuous correlation between solar wind properties and relativistic electron population in the Earth's magnetosphere [12,13]. They noted the important role the southward turning of the interplanetary magnetic field (IMF) plays in the process, with northward turning providing insignificant contribution in the modulation of the relativistic electron population by the high-speed solar wind and the leading pressure pulse. The role of the southward turning of the IMF has been studied by Baker et al. (1998) [14]. Baker et al. (1998) argued that the relativistic electron population is seeded by the electrons in the energy range of a few hundred KeV, which are introduced to the magnetosphere by the sub-storm injections associated with the southward turning of the IMF [14]. Reeves et al. (2011) repeated the analysis of Paulikas & Blake (1979) with a longer dataset from 1989 to 2010 and reported a more complex relationship between radiation belt electron fluxes and solar wind velocities than the linear relationship hinted by the previous statistical studies [15]. Particularly, they uncovered a triangular distribution of the electron fluxes with respect to the solar wind velocities. There were a velocity-dependent lower limit and a velocity independent upper limit for the electron fluxes in contrast with that predicted by an assumption of linear correlation between solar wind velocity (Vsw) and the logarithm of the electron fluxes [15]. Belian et al., 1996 examined electron flux data from 1979 to 1994, it's shown that high energy electron fluxes (E >300 keV) showed a cycle of 11 years. Also, they showed the relativistic electron cycle is out of phase with the sunspot cycle as electrons showed a minimum rate at the solar maximum instead of peaking [16]. Reeves (1998) analyzed the 30 most intense relativistic electron events from 1992 to 1995 in the transition period from solar maximum to solar minimum and discovered that every relativistic electron enhancement was associated with a magnetic storm and concluded that there is a low correlation between the strength of the magnetic storm and the strength of the relativistic electron flow [17]. The question of which magnetic storms produce relativistic electrons was further investigated by O'Brien et al. (2001) using cross-correlation analysis to determine which parameters of the solar wind influence the flux of relativistic electrons and found that sustained high solar wind velocity and long-duration ULF wave activity are more likely to be important mechanisms for electron flux enhancements than the sub-storms or VLF waves determined by the AE index [18]. The acceleration of relativistic electrons has been widely studied, but the mechanisms for electron loss during geomagnetic storms are also of particular interest. The decrease in the electron flux associated with the 'Dst effect' was studied by Kim & Chan (1997) and involves a temporary adiabatic dropout in electron fluxes [19]. Reeves et al. (2003) analyzed 276 geomagnetic storms between 1989 and 2000 and confirmed that geomagnetic storms can either increase or decrease electron fluxes in the radiation belts, also no correlations between the pre-storm and post-storm electron fluxes were reported [20].

Using correlation analysis, Lyatsky and Khazanov investigated the effect of solar wind density and solar wind velocity upon the relativistic electron population (>2 MeV) at geostationary orbit [21]. They found that the electron fluxes increase for higher solar wind speeds and decrease for increasing solar wind densities. Their results are consistent with results from Onsager et al. (2007), who had reported that an abrupt increase in solar wind densities can contribute to relativistic electron loss [22]. Lyatsky & Khazanov (2008) also reported that solar wind speeds display correlation with electron fluxes after two days like previously known, but solar wind densities show the best correlation with electron fluxes after about 15 hours and stressed the strong influence of solar wind density rather than just solar wind velocity upon the relativistic electron fluxes [21].

Although the various studies on radiation belt and relativistic electron flux has been made, still the adequate research and study is needed for a proper understanding of the dynamics of the radiation belt and factors that enhance the relativistic electrons. The observation of radiation belt and relativistic electron flux is always necessary because it has a direct impact on satellite technology, the health of astronauts, and space weather phenomena. Thus, we have realized to study the pattern of relativistic electron flux on geostationary orbit and other probable factors that affect it. In this paper, we will show the correlation of relativistic electrons with different solar parameters (sunspot number, solar flux and solar wind parameters) using 27 days averaged data of 24 years (1996- 2020). The study covers two solar cycles- solar cycle 23 and solar cycle 24. The paper is organized as follows: In section 2, we have described the data set and methodology of our work. In section 3, we have presented our results and discussion. Finally, we have concluded our findings in section 4.

2. DATA SET AND METHODOLOGY

In this study, the internet-based supply of data supplied by OMNI (Operating Mission as Nodes on the Internet) and NOAA (National Oceanic and Atmospheric Administration) has been used. OMNI database (https://www.omniweb.gsfc.nasa.gov) provides near-Earth solar wind magnetic field and plasma parameter data from several spacecraft in geocentric orbits. NOAA is the American scientific agency that monitors Earth systems, manages the data collection network, and conducts scientific research on the oceans and atmosphere. Under

NOAA's space weather monitoring mission, it has operated a series of GOES (Geostationary Operational Environmental Satellites) with Space Environment Monitor (SEM) instrument subsystem since 1974 [23]. The SEM is continuously providing Energetic particles and soft x-ray data, which is made available by NOAA's National Environmental Satellite Data and Information Service division through GOES data access link https://www.ngdc.noaa.gov/stp/satellite/goes/dataac cess.html. To date, 17 GOES satellites have been launched and currently four GOES satellites are in operational use, whereas the other 13 satellites in geostationary orbit are inactive or repurposed [24].

From the OMNI system, we have made use of 27-days resolution data observation of Vsw, Nsw, IMF-Bz, R, F10.7, and Tsw. Whereas from NOAA's database, we have made the 1-minute interval data observation of relativistic electron fluxes with energies >0.8 MeV, >2MeV and >4 MeV. Later this observation was converted to a 27-day resolution by taking the average of 1-minute resolution data of 27 days. The observation period is chosen for 24 years, from 1996 to February of 2020, which includes solar cycle 23 (1996-2007) and solar cycle 24 (2008-2019). We have applied cross correlation and wavelet analysis techniques to observe the variation of electron flux in geostationary orbit with time and to evaluate the correlation between relativistic electron flux and other OMNI parameters respectively.

2.1 Cross- Correlation

Cross correlation is the multi-time scale, statistical tool used to understand the level of relationship among different variables along with time-delay analysis and extracts the analogous nature relative to each other in time to scout out the new information [25, 26]. The correlation coefficient ranges from -1 to +1 and the coefficient value around ±1 explains high correlation, whereas around zero reflects a moderate or poor correlation between the compared parameters [27, 28]. The cross-correlation coefficient is plotted against time (years, in this paper) which helps to find out the lead or lag between the comparable indices after establishing their correlation [29].

2.2 Wavelet Analysis

Wavelet analysis is used to analyze changes in variance where we can determine dominant modes of variability and how these modes vary in time by decomposing time series into time-frequency space [30]. As, the signals are dynamic over time we have used Continuous Wavelet Analysis in our work.

Continuous Wavelet Transforms (CWT) can provide the time-frequency representation of the signal [31]. To extract the information about the behavior of the system, the local time-frequency energy density of a signal can be observed on a wavelet scalogram. Scalogram is a tool for wavelet analysis, which is obtained by taking the squared modulus of the wavelet coefficients [30].

Various researchers have used wavelet analysis tools in their work. Katsavrias et al. (2012) performed wavelet and Lomb-Scargle periodogram analysis of the time series data of solar wind parameters and magnetospheric indices to verify short-term, annual, semi-annual and intermittent periodicities observed in solar activity [32]. Adhikari et al. (2018) utilized wavelet analysis to study Polar Cap Voltage (PCV) and field-aligned currents [29]. Khanal et al. (2019) employed CWT analysis to study spectral characteristics of geomagnetically induced currents (GICs) associated with high-intensity long-duration auroral-electrojet activities [33]. The detailed explanation of the theory associated with CWT can be found in various papers [25, 30]. According to the theory, we have programmed all the algorithms in MATLAB selecting the Morlet wavelet function to obtain meaningful information about the relativistic electron flux in geostationary orbit through scalogram and Global Wavelet Spectrum (GWS).

3. RESULTS AND DISCUSSIONS
3.1 Time Series analysis

Figure 1 represents the time series plot for the year 1996 to 2020 of 27 days averaged electron flux (>0.8 MeV), electron flux (>2 MeV), electron flux (>4 MeV), plasma temperature (Tsw), the southern component of interplanetary magnetic field (IMF-Bz), plasma density (Nsw), solar wind velocity (Vsw), solar flux (F10.7) and sun spot number (R) respectively from top to bottom.

1996-2020
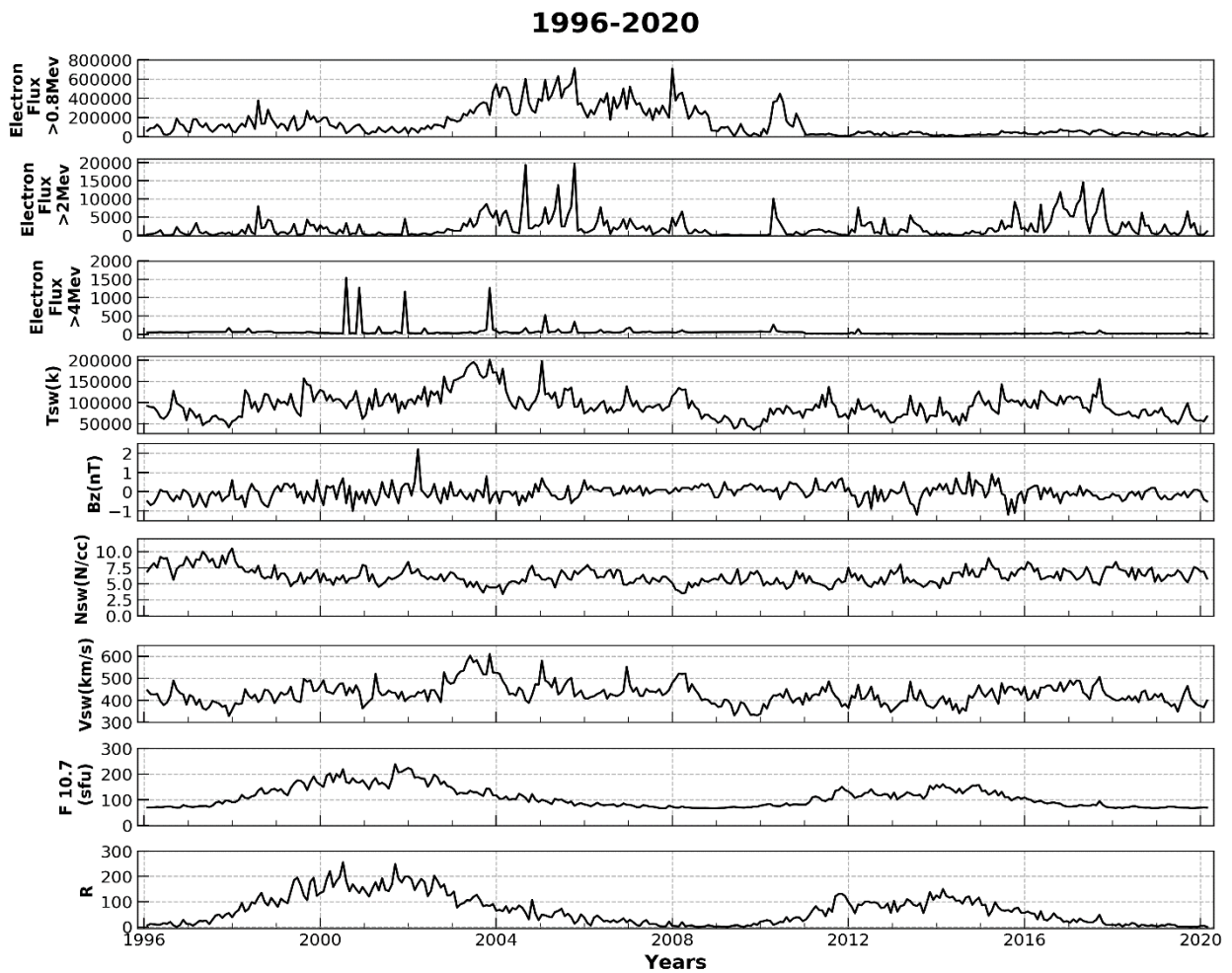
Fig. 1: Variation of the solar parameters- R, Vsw (km/s), Nsw (N/cc), Bz (nT), Tsw (nT) and Electron flux (>0.8 MeV, >2MeV, >4MeV) during the year 1996 to 2020.

The figure showed that the relativistic electron flux >0.8 MeV has reached the maximum value of around 750000 e/ (cm^2 s sr) during the years 2005 and 2008. Whereas relativistic electron flux >2MeV has gained the maximum value around 20000 e/ (cm^2 s sr) during the end of 2004 and 2005. Similarly, a peak value around 15000 e/ (cm^2 s sr) of flux >2Mev is also observed during the years 2016 and 2017. The relativistic electron flux >4 Mev has the peak count in the years 2000, 2002 and 2004 i.e., during the mid-years of solar cycle 23 (1996-2008). If we analyze the plots according to the solar-cycle, we observed the maximum value of relativistic electron flux in solar-cycle 23 (1996-2008) in comparison to solar cycle 24 (2009-2020). Plasma temperature was measured around 50000 k in some years and the maximum value at around 200000 k was measured in 2003 and 2005. Similar variance to plasma temperature was also shown by the velocity of solar wind. It gained the maximum value of 600 Km/s during in 2003 and beginning of 2005. During the initial year of solar cycle 23 (1996), sunspot numbers were zero and later showed a rise over the years and reached a maximum value of about 300 during 2000 to 2002 and decreased again to zero during 2008, that is the end of solar cycle 23. We recorded fewer sunspot counts at the beginning of solar cycle 24, which was later increased to over 100 from 2012 to 2014, and again counted zero at the end of 2019, that is the end of solar cycle 24. Solar flux (F10.7) with a minimum value of 90 sfu at the beginning of solar cycle displayed a similar variation as that of the sunspot number and reached a maximum value of around 250 sfu in 2003 and around 150 sfu in 2014. The curve of plasma density ranged from a maximum value of 11 N/cc to a minimum value of 2.5 N/cc. During the period 1996-2020, the continuous variation between between -1 nT to 2 nT of IMF-Bz was observed.

As per the result reflected by time series plots, the outer radiation belt in the magnetosphere is occupied mostly by relativistic electrons of energy less than 4 MeV. Also, it depicts that low relativistic electron flux is counted during the increasing phase of the solar cycle. But the plots are not sufficient to establish the relation between the relativistic electron flux and the solar parameters. Hence, we have used the statistical methods: cross- correlation analysis and wavelet analysis method in this study.

3.2 Cross- Correlation

Figure 2(a) shows the cross-correlation of the relativistic electron flux of energy greater than 0.8

MeV with a southward component of IMF (Bz), solar wind temperature (Tsw), Plasma density (Nsw), solar wind velocity (Vsw), sunspot number (R) and solar flux (F10.7) of the year 19996 to 2020 (includes solar cycle 23 and solar cycle 24).
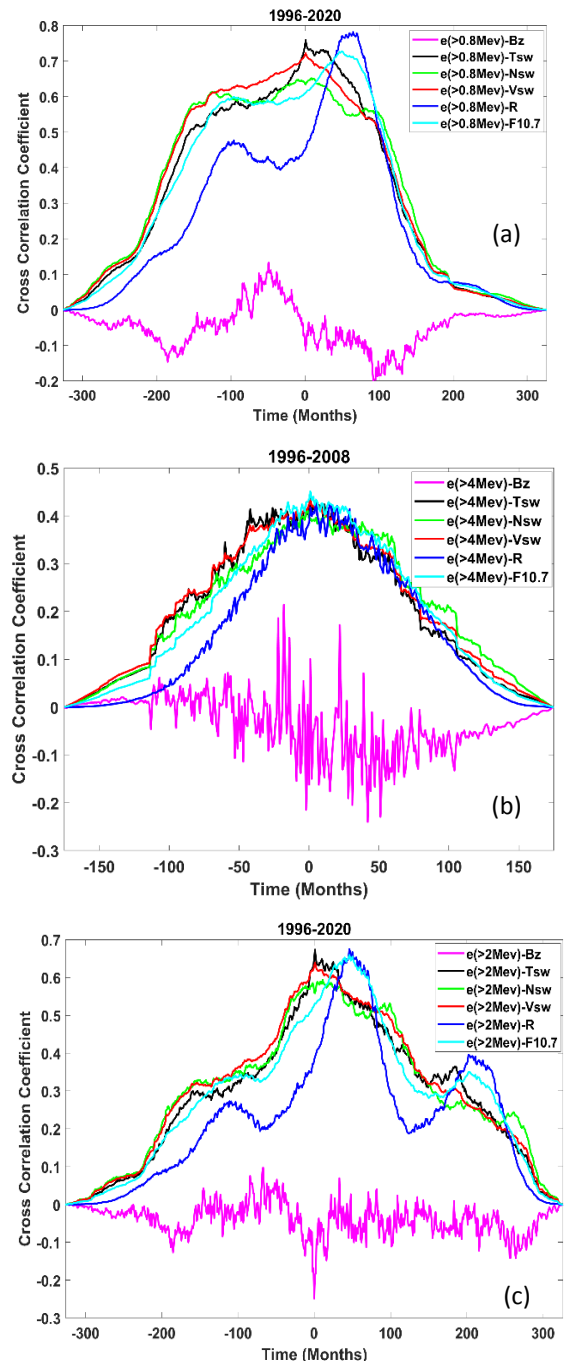

Fig. 2: Representation of cross-correlation coefficient in time (months) of relativistic electrons flux of (a) energy >0.8 MeV (b) energy >2 MeV (c) energy >4 MeV for year 1996-February 2020 with southern component of IMF(Bz), Plasma Temperature(Tsw), Plasma density(Nsw), Solar wind velocity(Vsw), Sunspot number(R) and solar flux (F10.7)

P. Poudel, N. Parajuli, A. Gautam, D. Sapkota, H. Adhikari, B. Adhikari, A. Silwal, S. P. Gautam, M. Karki, R. K. Mishra

In the figure the red (e >0.8meV-Vsw) shows the peak at 0.7 and black (e >0.8MeV-Tsw) at 0.75 at zero-time lag. Which means when Vsw and Tsw are in phase, they are highly and positively correlated with relativistic electron flux having energy greater than 0.8 MeV. The green (e >0.8MeV-Nsw) curve also showed a similar nature as red and black curves, with a maximum value of 0.65 at a zero-time lag. This also manifests good correlation of electron flux >0.8MeV with plasma density when they are in phase. The blue curve (e >0.8MeV-R) also showed the good positive correlation coefficient of 0.8 at a time lag of +80 months. The nature of blue curve can be described as sunspot number and solar flux leads electron flux by 80 months after they get correlated [29]. Similar nature as that of blue is shown by the cyan (e >0.8MeV-F10.7) but with maximum correlation peak of 0.7 at +80- time lag. But the magenta (e >0.8MeV-Bz) curve showed unusual and unsymmetrical nature as compared to other curves. The curve, crossed the zero at around a time lag of –45 months showing positive correlation of 0.1 and again reached the maximum negative correlation coefficient value of -0.3 at time lag +100 months. Thus, it can be summarized as the moderate correlation of southward component of the interplanetary magnetic field with relativistic electron flux of energy >0.8MeV.

Figure 2(b) shows the cross correlation of relativistic electron flux of energy greater than 2 Mev with Bz, Tsw, Nsw, Vsw, R and F10.7 of the year 1996 to 2020. Here the green (e >2Mev-Nsw), Black (e >2Mev-Tsw) and red (e >2Mev-Vsw) curves almost overlapped throughout the time series, but with peak correlation coefficient value of 0.57, 0.65, and 0.62 respectively at 0-time lag indicated the good positive association of Nsw, Vsw and Tsw with relativistic electron flux of energy >2MeV. Similarly, the blue curve (e >0.8Mev-R) and cyan curve (e >2Mev-F10.7) also showed the positive correlation of sunspot number with relativistic electrons of energy >2Mev but with a maximum correlation coefficient of 0.6 at a time lag of +70 months. This reveals that sunspot number leads electron flux before they get correlated. Similar to the nature shown in figure 2(a), the magenta curve (e >0.8Mev-Bz) showed unsymmetrical behavior crossing the zero several times within the vicinity +1 and -0.25. Hence can be considered as the moderate correlation of Bz with electron flux >2Mev.
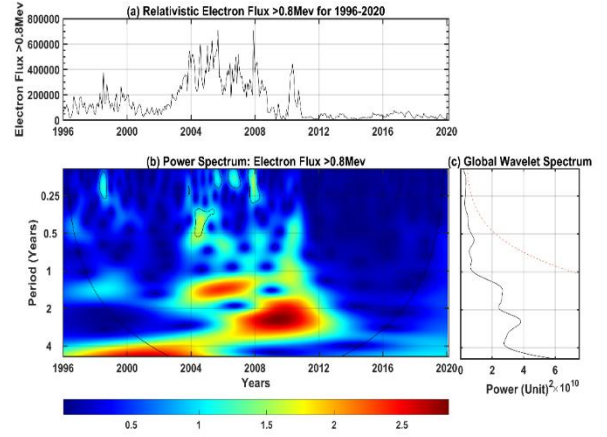
Fig. 3: (a) Relativistic electron flux of energy >0.8 Mev recorded from 1996 to 2020 (b) Power Spectrum of flux with the color scaled bar and (c) Global Wavelet Spectrum showing the main periodicities.
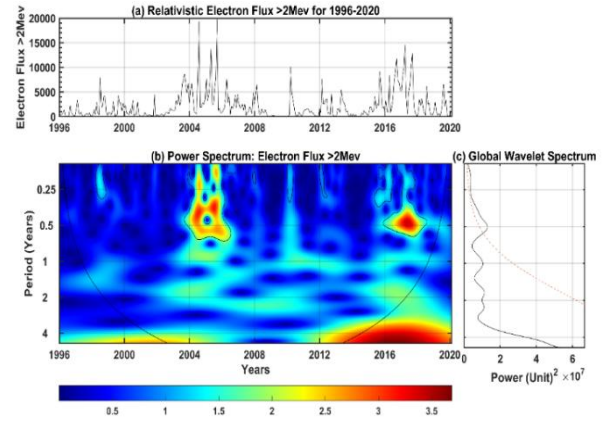
Fig. 4: (a) Relativistic electron flux >2 Mev recorded from 1996 to 2020 (b) Power Spectrum of flux with the color scaled bar and (c) Global Wavelet Spectrum showing the main periodicities
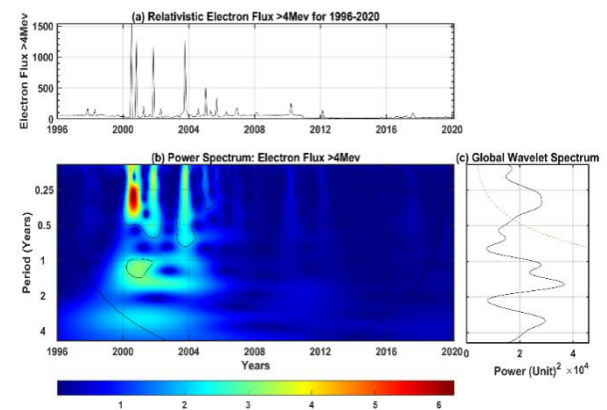
Fig. 5: (a) Relativistic electron flux >4 Mev recorded from 1996 to 2020 (b) Power Spectrum of flux with the color scaled bar and (c) Global Wavelet Spectrum showing the main periodicities.

Figure 3(c) with the horizontal axis representing the time series ranging from -326 to +326 months represents the cross-correlation coefficient of the relativistic electron flux of energy greater than 4MeV with Bz, Vsw, Tsw, Nsw, R, and F10.7 for the years 1996-2020. The figure described the good positive correlation of electron flux >4MeV with Tsw, Vsw and Nsw showing the maximum positive correlation coefficient of 0.4 at time lag 0 i.e. at phase. The blue curve (e >2MeV-R) also showed a good positive correlation of electron flux with a sunspot number accompanied by a maximum correlation coefficient value of 0.4 at a time lag of 0-months. The nature of the magenta curve (e >2MeV-Bz) described the moderate correlation of Bz with electron flux >4MeV as it reached the maximum positive correlation of 0.18 at a time lag of -50 month and also the maximum negative correlation coefficient value of -0.2 at a time lag of -150 months.

3.3 CWT analysis

To study the periodicities of relativistic electrons we apply wavelet analysis. Figures 3, 4, and 5 present the results of CWT. The peak contours regions seen in the power spectrum comprise a confidence level of more than 95% which concerns red noise processing levels [32]. To establish the null hypothesis for the significance of power regions in wavelet spectrum Red noise leveling is important [29]. We have set the lag 1 autocorrelation coefficient of 0.72 for construction of red noise. The red dotted line in GWS (Figure 3(c), 4(c), 5(c)) corresponds to red noise spectrum. The vertical plane in the scalogram (Figure 3(b), 4(b), 5(b) is the time in years and the horizontal plane is the period in the year. Dealing with finite-length time series makes an error to occur at edges of wavelet power spectrum [29]. To overcome this, we padded the time series with appropriate zeros. This method of adding zeros, however, creates discontinuities at the edges of the time series, which is solved by inserting a cone of influence (represented in the figures with U-shaped black lines). The edge effects are negligible beyond the cone of influence [29]. The peaks observed in the GWS plot show the main periodicities associated with the relativistic electron flux in the period of 1996 to 2020.

It is clear from the figures, flux >0.8MeV and >2MeV frequencies can be observed in both higher and lower frequency regions whereas electron flux >4MeV have values in higher frequency regions only. According to the figure 3(b) relativistic

electrons >0.8MeV periodicities is confined in the regions ~ 1-4 and below 4 years. Contrarily, in case of relativistic electrons >2MeV and >4MeV periodicities are observed between the regions 0-0.75, below 4 and 0-0.5, 1-2 year. Evidently, from Global Wavelet Spectrum (GWS), the main periodicities lie between the ~1.3, 2.2, 4.1 years with corresponding energies ~2.5, 3.8, 6 $\times 10^3$ (units)^2 respectively for electrons >0.8 Mev. On the other hand, the main periodicities: ~ 0.5, 1, 2.7, 4.1 and 1.6, 1.5, 1.5, 5 with corresponding energies ~0.30, 0.6, 1.1, 1.8, 3.8, 4.1 and 2.9,1.8, 2.6, 3.8, 2.9, 1.9×10^3 (Unit)^2, for electrons >2MeV and >4MeV respectively.

Results from figure 3,4 and 5 displayed that the power spectrum in case of relativistic electron in the range >0.8MeV and >2MeV have more variation in energy in comparison to power spectrum of relativistic electron in the range >4MeV which coherently prop up the results of time series analysis.

4. CONCLUSIONS

Various parameters associated with solar activities have an influence in the space weather phenomena and space technology. Solar phenomena have a major contribution to the formation of radiation belt in the upper atmosphere. In this work, we have studied the correlation between the relativistic electron flux of different energy and parameters associated with solar activities i.e. sunspot numbers, solar flux and solar wind parameters by using cross-correlation technique and wavelet analysis. Based on the obtained results, we have made the following conclusions.

1. Within the period 1996-2020, the time series plot showed the peak value of relativistic electron flux with energy >0.8MeV during 2005-2008, flux >2MeV in 2004 and 2005, flux >4MeV during 2001 and 2003. Similar energy distribution was also observed from the scalogram. This suggests that solar cycle 23 (1996-2008) produced more intensity of relativistic electron flux than solar cycle 24 (2009-2020). Also, the highest electron flux count of relativistic electron flux of energy >0.8MeV and >2MeV in comparison to flux >4MeV reveals that outer radiation belt of Earth's magnetosphere comprises mostly of relativistic electrons of energy less than 4MeV.

2. Cross-correlation plots illustrated that the electron flux >0.8MeV and electron flux >2MeV have a good positive association with

solar wind velocity (Vsw), plasma density (Nsw), temperature (Tsw), sun spot number (R), and solar flux (F10.7) with correlation coefficient around 0.7. The relativistic electron flux >4MeV showed a positive association with above mentioned solar parameters but the coefficient value was only ~0.4. This concludes that there is a greater contribution of solar activity and solar parameters to produce and influence electron flux of energy between 0.8 and 4MeV, than that of flux >4MeV.

3. The southern component of interplanetary magnetic field (Bz) did not show any perfect correlation with relativistic electron flux as it had crossed the zero of cross-correlation plot several times showing a positive and negative correlation in an irregular pattern, which reveals that it does not have any specific association and have no significant effect on the enhancement of relativistic electron flux.

4. Results from wavelet analysis showed the higher periodicity of electron flux of energy >0.8MeV which describes the greater energy variation of relativistic electrons of range >0.8MeV in comparison to flux of energy >2Mev and energy >4MeV.

ACKNOWLEDGEMENTS

REFERENCES

[1] Cline, T. L. and McDonald, F. B. Relativistic electrons from solar flares. *Solar Physics*, **5**(4): 507–530, (1968).

[2] Mauk, B. H.; Fox, N. J.; Kanekal, S. G.; Kessel, R. L.; Sibeck, D. G.; & Ukhorskiy, A. Science Objectives and Rationale for the Radiation Belt Storm Probes Mission. *Space Science Reviews*, **179**(1-4): 3–27, (2012).

[3] Van Allen Radiation Belt. Available online: https://en.wikipedia.org/wiki/Van_Allen_radiatio n_belt (Accessed on 1 January,2021)

[4] Baker, D. N. Satellite Anomalies due to Space Storms. *Space Storms and Space Weather Hazards*, 285–311 (2001).

[5] Li, W. and Hudson, M. K. Earth's Van Allen Radiation Belts: From Discovery to the Van Allen Probes Era. *Journal of Geophysical Research: Space Physics,* **124**(11): 8319-8351, (2019).

[6] Miyoshi, Y. and Kataoka, R. Probabilistic space weather forecast of the relativistic electron flux enhancement at geosynchronous orbit. *Journal of Atmospheric and Solar-Terrestrial Physics*, **70**(2-4): 475–481 (2008).

[7] Reeves, G. D. Relativistic electrons and magnetic storms: 1992-1995. *Geophysical Research Letters*, **25**(11): 1817–1820 (1998).

[8] Ukhorskiy, A. Y. and Sitnov, M. I. Dynamics of Radiation Belt Particles. *Space Science Reviews*, **179**(1-4): 545–578 (2012).

[9] Meyer, P. and Vogt, R. The primary cosmic-ray electron flux during a Forbush-type decrease. *Journal of Geophysical Research*, **66**(11): 3950–3952 (1961).

[10] Sakurai, K. On the relativistic electrons in the solar atmosphere. *Journal of geomagnetism and geoelectricity*, **12**(2): 70-76 (1961).

[11] Satio, H. and Kitao, K. Energy loss of a charged particle traversing ionized gas and injection energies of cosmic rays. *Progress of Theoretical Physics*, **16**(2): 139-148 (1956).

[12] Paulikas, G. A. and Blake, J.B. Effects of the solar wind on magnetospheric dynamics: Energetic electrons at the synchronous orbit. *Geophysical Monograph Series*, **21**: 180-202 (1979).

[13] Blake, J. B.; Baker, D. N.; Turner, N.; Ogilvie, K. W. and Lepping, R. P. Correlation of changes in the outerzone relativistic-electron population with upstream solar wind and magnetic field measurements, *Geophysical Research Letters*, **24**(8): 927-929 (1997).

[14] Baker, D.; Li, X.; Blake, J. and Kanekal, S. Strong electron acceleration in the Earth's magnetosphere, *Advances in Space Science*, **21**(4): 609–613 (1998).

[15] Reeves, G. D. *et al.* On the relationship between relativistic electron flux and solar wind velocity: Paulikas and Blake revisited. *Journal of Geophysical Research: Space Physics*, **116**(A2): (2011).

[16] Belian, R. D. *et al.* Relativistic electrons in the outer-zone: An 11-year cycle; Their relation to the solar wind. *AIP Conference Proceedings*. **383**(1): (1996).

[17] Reeves, G. D. Relativistic electrons and magnetic storms: 1992–1995. *Geophysical Research Letters*, **25**(11): 1817– 1820 (1998).

[18] O'brien, T. P.; Mcpherron, R. L.; Sornette, D.; Reeves, G. D.; Friedel, R. & Singer, H. J. Which magnetic storms produce relativistic electrons at geosynchronous orbit? *Journal of Geophysical Research: Space Physics*, **106**(A8): 15533-15544 (2001).

[19] Kim, H. and Chan, A. A. Fully adiabatic changes in storm time relativistic electron fluxes. *Journal of Geophysical Research: Space Physics,* **102(A10)**: 22107-22116 (1997).

[20] Reeves, G. D.; Mcadams, K. L.; Friedel, R. H. and O'brien, T. P. Acceleration and loss of relativistic electrons during geomagnetic storms. *Geophysical Research Letters,* **30**(10): (2003).

[21] Lyatsky, W. and Khazanov, G. V. Effect of solar wind density on relativistic electrons atgeosynchronous orbit. *Geophysical Research Letters,* **35**(3): ..... (2008).

[22] Onsager, T. G.; Green, J. C.; Reeves, G. D. and Singer, H. J. Solar wind and magnetospheric conditions leading to the abrupt loss of outer radiation belt electrons. *Journal of Geophysical Research: Space Physics,* **112**(A1): .... (2007).

[23] National Centers for Enviromental Information. Available Online: www.ngdc.noaa.gov/ngdcinfo/aboutngdc.html (accessed on 20 october,2020)

[24] Wikipedia- Geostationary Operational Environmental Satellite (accessed on 20 October, 2020).

[25] Usoro, A. E. Some basic properties of cross-correlation functions of n-dimensional vector time series, *Journal of Statistical and Econometric Methods,* **4**(1): 63–71 (2015).

[26] Adhikari, B.; Baruwal, P. & Chapagain, N. P. Analysis of super-sub storm events with reference to polar cap potential and polar cap index. *Earth and Space Science,* **4**(1): 2–15 (2017a).

[27] Katz, R. W. Use of cross correlations in the search for teleconnections. Journal of Climatology, **8**(3): 241–253 (1988).

[28] Adhikari, B.; Dahal, S. and Chapagain, N. P. Study of field-aligned current (FAC), interplanetary electric field component (Ey), interplanetary magnetic field component (Bz) and northward (x) and eastward (y) components of geomagnetic field during supesubstorm. *Earth and Space Science,* **4**(5): 257–274 (2017b).

[29] Adhikari, B.; Dahal, S.; Sapkota, N.; Baruwal, P.; Bhattarai, B. and Chapagain, N. P. Field Aligned Current and Polar Cap Potential and Geomagnetic Disturbances: A Review of Cross-Correlation Analysis. *Earth and Space Science,* **5**: 440-455 (2018).

[30] Torrence, C. & Compo, G. P. A Practical Guide to Wavelet Analysis. *Bulletin of the American Meteorological Society,* **79**(1): 61–78 (1998).

[31] Bialasiewicz, J. T. Application of Wavelet Scalogram and Coscalogram for Analysis of Biomedical Signals, *Proceedings of the World Congress on Electrical Engineering and Computer Systems and Science,* 333: ..... (2015).

[32] Katsavrias, C.; Preka-Papadema, P. & Moussas, X. Wavelet Analysis on Solar Wind Parameters and Geomagnetic Indices. *Solar Physics,* **280**(2): 623-640 (2012).

[33] Khanal, K.; Adhikari, B.; Chapagain, N. P. & Bhattarai, B. HILDCAA-related GIC and possible corrosion Hazard in underground pipelines: A comparison based on wavelet transform. *Space Weather,* **17**: 238–251 (2019).